Kok Kwong Ngoi and Hieng Kiat Jun*

Study of fabrication of fully aqueous solution processed SnS quantum dot-sensitized solar cell

https://doi.org/10.1515/gps-2019-0012
Received June 28, 2018; accepted November 13, 2018.

Abstract: In this prelimnary work, the aim was to fabricate a simple tin (II) sulfide (SnS) quantum dot-sensitized solar cell (QDSSC) from aqueous solution. The SnS QDSSCs were characterized by using current-voltage test (I-V test), scanning electron microscopy (SEM), and ultraviolet-visible (UV-Vis) spectroscopy. SEM results showed the presence of TiO_2 and SnS elements in the sample, confirming the successful synthesis of SnS quantum dots (QDs). The overall efficiency of QDSSCs increased when concentration of the precursor solutions, which were aqueous sodium sulfide and tin (II) sulfate decreased from 0.5 M to 0.05 M. On the other hand, for a fixed precursor concentration, the efficiency of QDSSC reduced once an optimal cycle of of successive ionic layer adsorption and reaction (SILAR) was achieved. The bandgap energies of QDs obtained by extrapolating the Tauc plot were used to predict the QDs size. In general, the QD size was bigger for samples prepared from precursor concentration of 0.5 M, and with higher number of SILAR cycle used. The best performance was obtained from sample prepared from 0.05 M precursor concentration with 4 SILAR cycles.

Keywords: quantum dot-sensitized solar cell; SnS; SILAR; bandgap

Abbreviations:

CBD	Chemical bath deposition
FF	Fill factor
FTO	Fluorine-doped tin oxide
I-V	Current-voltage
QDs	Quantum dots
QDSSC	Quantum dot-sensitized solar cell
SEM	Scanning electron microscopy
SILAR	Successive ionic layer adsorption and reaction
SnS	Tin (II) sulfide
UV-Vis	Ultraviolet-visible
V_{OC}	Open-circuit voltage
J_{SC}	Short-circuit current density

*** Corresponding author: Hieng Kiat Jun,** Department of Mechanical and Material Engineering, Lee Kong Chian Faculty of Engineering and Science, Universiti Tunku Abdul Rahman, Bandar Sg. Long, 43000 Kajang, Malaysia, e-mail: junhk1@gmail.com
Kok Kwong Ngoi, Department of Mechanical and Material Engineering, Lee Kong Chian Faculty of Engineering and Science, Universiti Tunku Abdul Rahman, Bandar Sg. Long, 43000 Kajang, Malaysia

1 Introduction

Solar energy is one of the clean and renewable energy technologies available in the world. Compared with current main energy sources, i.e. fossil fuel such as crude oil, coal, and natural gas, it produces no harmful substances to the environment. Solar energy will never be depleted as long as the sun is available. Solar cells function by harvesting the sunlight, and converting it into electricity [1].

In 1954, the first generation of solar cell was made in Bell Laboratories by forming a diffused silicon p-n junction [2]. Silicon was chosen because of the availability and the popularity in semiconductor industry. However, these silicon-based solar cells are expensive to produce. The second generation of solar cells are known as thin film solar cells, which have similar working principle as the first generation solar cells. Thin film solar cells are aimed for mass production. However, deposition of thin film requires high temperature and high vacuum condition which cause high production cost of thin firm solar cells [3]. The combination of knowledge and experience acquired from the first and second generation of solar cells has become the foundation for the third generation solar cells to achieve lower production cost and high energy efficiency which can exceed the theoretical Shockley-Queisser limit of 33% [4,5]. Solution-processed semiconductor solar cells such as dye-sensitized solar cells and quantum dot-sensitized solar cells (QDSSC) are catergorized as third generation solar cells [1].

Typically, QDSSC consists of photoelectrode, electrolyte, and counter electrode. The photoelectrode consists of conducting glass coated with wide band gap semiconductor, usually titanium dioxide (TiO_2) or zinc oxide (ZnO), with semiconductor quantum dots (QDs)

attached on it. Commonly used material for counter electrode is platinum (Pt), but other materials like copper (I) sulfate (Cu_2S) is also used. QDs are nano-sized particles that are responsible for the light absorbance and generation of electron-hole pairs. The generated excited electrons will then be transfered to the wide band gap semiconductor and ultimately to the external circuit. QDs with small sizes can lead to quantum confinement effect, where the bandgap values of the QDs change accordingly. This effect is beneficial as the response to light can be tuned based on specific bandgap and QD's size. Many semiconductor materials such as SnS, CdS, CdSe, and PbS have been identified for sensitizing solar cell application [6,7].

Materials such as CdS, CdSe, and PbS have been commonly researched in the field of QDSSCs due to good optical properties. However, these materials show high toxicity that bring harms to the living creatures and environment, which are inconsistent with the main purpose of solar cells as a clean and green energy generator. On a bright side, few researches have demonstrated the application of SnS in QDSSCs. SnS is cheap and less toxic as compared with the materials mentioned above. SnS has been identified as a potential material for solar cells due to its low bulk bandgap of 1.09-1.30 eV and high conductivity and absorption coefficient. Besides, Sn and S are abundant on earth.

On the fabrication method of QDs, solution processed method like successive ionic layer adsorption and reaction (SILAR) is frequently employed. This method was first reported by Ristov et al. in 1985 [8]. SILAR method is basically an immersion of substrate in different cationic and anionic precursor solutions, and rinsing in deionized water for film growth purpose. The substrate must be rinsed after each dipping in precursor solution to washed away any unreacted ions. In general, SILAR method is an advanced version of chemical bath deposition (CBD) method. However, in CBD method, all the precursors are mixed together in one container, while in SILAR method, the precursors are separated. Thin film in SILAR method grows layer by layer, hence the film thickness can be controlled easily by varying the number of dipping cycle [9].

In this work, solution processed SnS QDSSCs were fabricated and investigated. Unlike previous reported studies, SnS was synthesized from SO_4^{2-} based salt as precursor, all in aqueous solution. The effect of concentration of precursor solution during the preparation of QDs was investigated. Besides, the number of dipping cycles on the efficiency QDSSC was also studied.

2 Materials and methods

2.1 Materials

Fluorine-doped tin oxide (FTO) conducting glass (13 Ω/sq.), titania paste and platinum precursor were purchased from Dyesol, Australia. Chemical reagents like $SnSO_4$, Na_2S and S were obtained from Sigma Aldrich, unless otherwise specified. All chemical reagents were used as received due to high purity grade.

2.2 Electrodes preparation

Anode electrodes were prepared by deposition of SnS QDs which were fabricated via SILAR technique. Prior to that, TiO_2 layer was deposited on the FTO glass via doctor blading method, which was then followed by sintering at 450°C for 30 min. The layer was prepared from titania paste, without dilution. The treated electrodes were then dipped into various concentrations of $SnSO_4$ and Na_2S acqueous solutions. Steps of SnS QDs deposition are described as below:

(a) Immersed electrode in $SnSO_4$ aqueous solution for 4 min.
(b) Rinsed electrode in deionized water for 1 min.
(c) Immersed electrode in Na_2S aqueous solution for 4 min.
(d) Secondary rinsing of electrode in deionized water for 1 min.

The above steps are regarded as 1 cycle. The steps were repeated for 0.05 M and 0.5 M precursor solutions, and from 2 to 6 cycles for each concentration of precursor solutions. Samples were numbered based on number of SILAR cycle. For example, A3 represents sample from set A prepared with 3 SILAR cycles. The complete samples ID are shown in Table 2.

As for the counter electrode, Pt-coated glass plate was prepared by spin coating Plastisol solution (or platinum precursor solution) onto a FTO conducting surface, followed by sintering at 450°C for 30 min.

2.3 Device assembly

After solution dipping and heat treatment, solar cell was assembled in sandwich type architecture with generic polysulfide liquid electrolyte. The electrolyte consisted of 1.0 M Na_2S and 0.1 M S in aqueous solution [10]. Parafilm

was used as spacer, where the centre of the film was cut out slightly larger than the area of the titania film before placing it on the substrate. Then electrolyte was added on top of the TiO_2/QDs film surface via pipette. Lastly, the photoanode and counter electrode were sandwiched and clamped together.

Materials characterizations were performed using scanning electron microscope (SEM) and ultraviolet-visible (UV-Vis) spectrophotometer. Device performance was validated with Keithley 2400 electrometer under light source at 1 sun. For SEM analysis, Hitachi S-3400N SEM was used to study the surface structure and morphology of the substrates. For UV-Vis analysis, model Cary 100 Conc. was used to analyze the QDs-sensitized substrate. The absorption rate of the samples was determined from the analysis.

3 Results and discussion

Three sets of QDSSC devices were fabricated from three different precursor concentrations (i.e. 0.05 M, 0.1 M and 0.5 M). These molarities were selected based on previous reported studies [11,12]. As these studies did not have a thorough investigation on the precursor optimization, we selected a set of general acceptable molarities which started from low molarity. We confined the study to a few precursor concentrations and capped it at 0.5 M. In each set, the anionic and cationic precursor concentrations were maintained at the same concentration level. For example, devices fabricated from 0.05 M were prepared from 0.05 M of $SnSO_4$ and 0.05 M Na_2S acqueous solution. The fabricated SnS-sensitized TiO_2 electodes exhibited a dark brown color as shown in Figure 1. With higher precursor concentration, the sensitized layer became black. The same observation is also true for higher SILAR cycles. In this work, the SILAR cycles were limited to maximum 6 cycles as more dipping cycles would result in QDs overloading [13,14].

The prepared QD-sensitized TiO_2 electrodes were then characterized with SEM imaging. Figure 2 shows the surface morphology of the fabricated TiO_2 and TiO_2/SnS layer of the electrode samples. TiO_2 was successfully deposited on the substrate, as porous structure of TiO_2

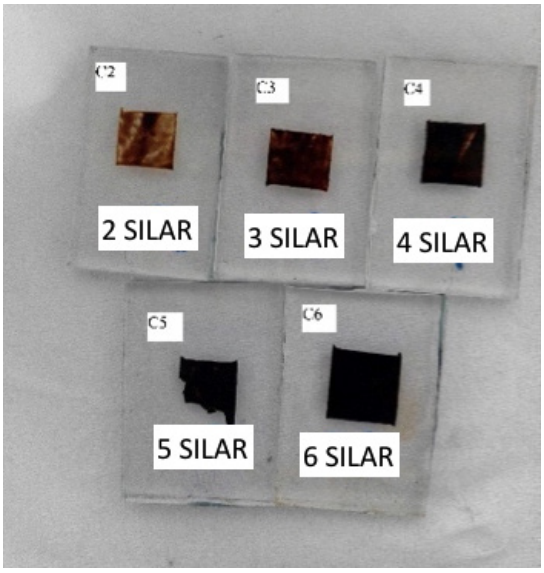

Figure 1: SnS QD-sensitized electrode sample. All samples show good film adhesion to the substrate despite irregular surface area.

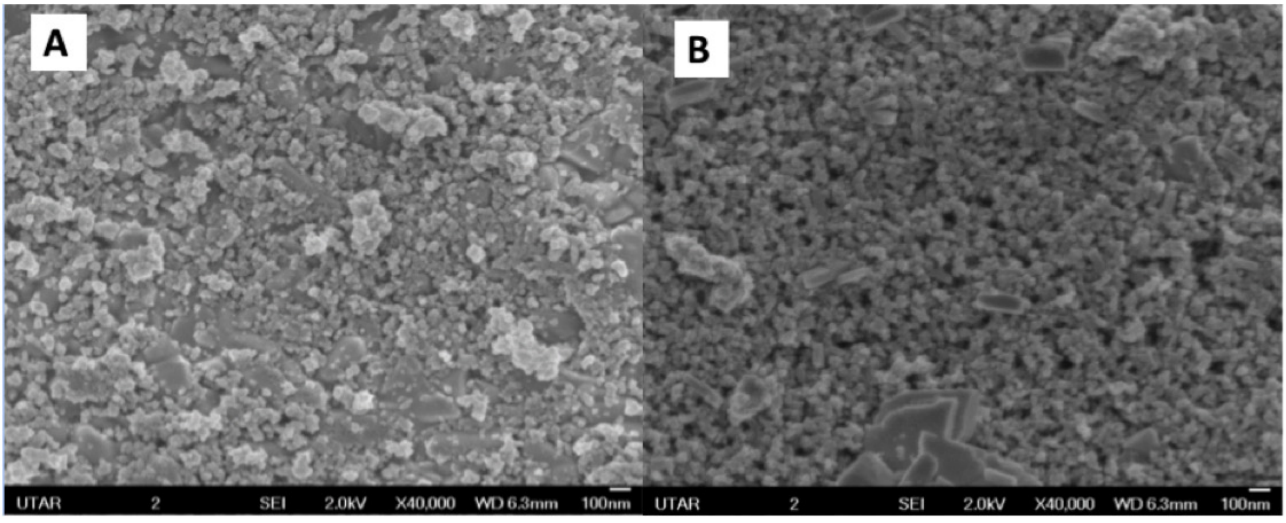

Figure 2: SEM micrographs of photoanode surface at 40,000x magnification. (a) Bare TiO_2 layer; (b) TiO_2/SnS layer.

nanoparticles was observed. The TiO_2 particles were also "sensitized" (or adsorbed) with SnS layer, where reduced porosity of the TiO_2 layer was observed. The porosity of the TiO_2 layer was determined qualitatively via Image-J software. The presence of Sn and S elements was also verified by EDX analysis on the same surface analysis (see Table 1 for elemental analysis). In the preparation steps of the TiO_2 layer, it is crucial to ensure no cracks are visible as such cracks will cause high shunt resistance, R_{SH} and lower the efficiency of the device [15].

The performances of the fabricated SnS QDSSCs are shown in Figure 3. The J-V curves of the individual SnS QDSSCs prepared from 0.05 M, 0.1 M and 0.5 M precursor concentrations are shown in Figures 3a-c, respectively.

Table 1: Elemental composition of sample TiO_2/SnS as detected via EDX analysis.

Element	Atomic %
Ti	16.42
O	81.95
Sn	0.98
S	0.65
Total	100.00

Meanwhile, Figure 3d depicts the performance trends of the sample sets. On the other hand, the performance parameters of the SnS QDSSCs are tabulated in Table 2, with information pertaining to the concentrations of precursor solution and SILAR cycles.

From the result obtained, for samples prepared from 0.05 M precursor solutions, the optimal number of dipping cycles is 4 cycles where the device exhibits the highest open-circuit voltage (V_{OC}), short-circuit current density (J_{SC}), and efficiency at 0.43 V, 0.40 mA/cm^2, and 0.07%, respectively, within the same group. The overall performance is still low compared to other types of QDSSC like CdS and CdSe. This could be due to the intrinsic optical properties of SnS itself [10,16,17]. The low performance was also confirmed by other research groups although some were able to achieve better result due to optimization done on the photoanode layer [11,12]. Further increasing the number of dipping cycles after 4 SILAR cycles does not show any significant improvement on the performance. In fact, the performance reduced dramatically with dipping cycles above 4 cycles. This could be attributed to the overloading of SnS QDs on the TiO_2 particles which subsequently increased the charge recombination rate at the TiO_2 interfaces [18]. At

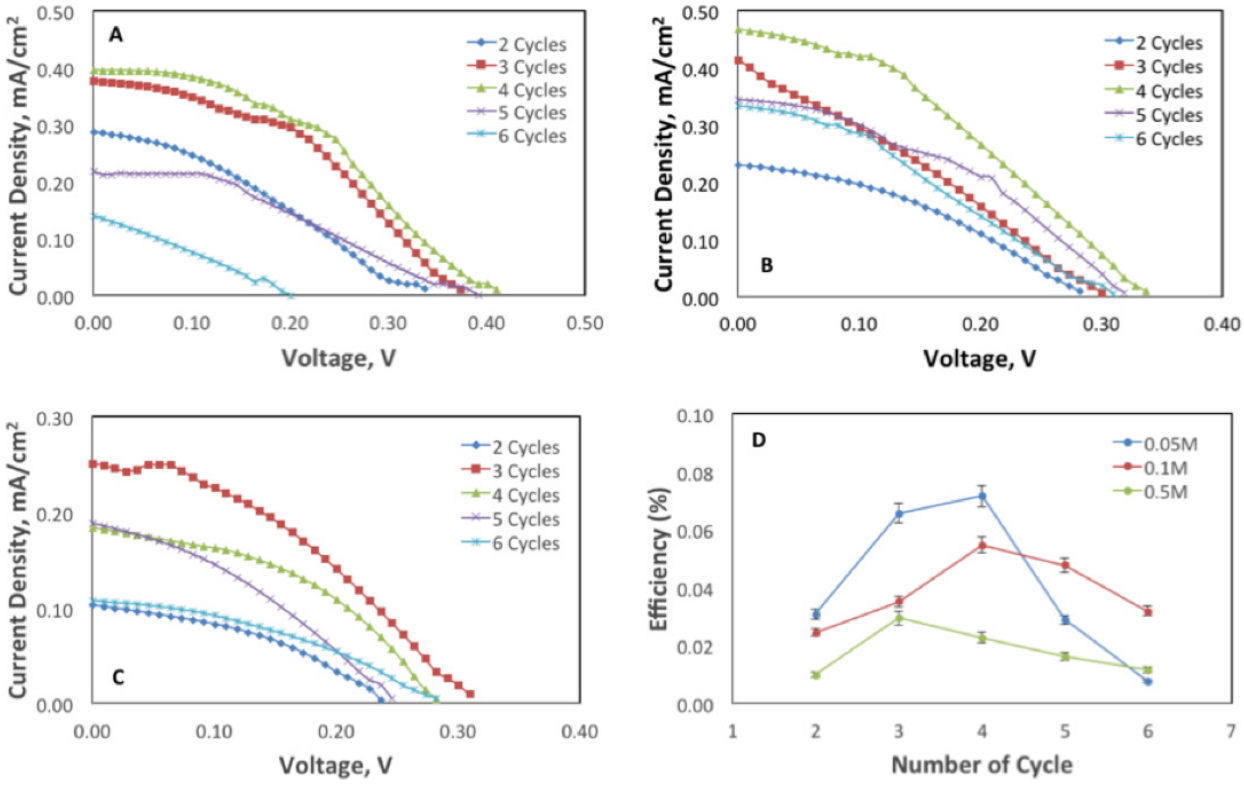

Figure 3: J-V curves for SnS QDSSC prepared from (a) 0.05 M precursor concentration; (b) 0.1 M precursor concentration; (c) 0.5 M precursor concentration with various dipping cycles. The efficiency trend is shown in (d).

Table 2: Relationship between concentration, number of SILAR cycles, and V_{OC}, J_{SC}, FF, and efficiency of SnS QDSSCs.

Concentration (M)	Sample ID	No. of cycle	Voc (V)	Jsc (mA/cm^2)	FF (%)	Efficiency (%)
0.05	C2	2	0.34	0.29	32.0	0.031
	C3	3	0.38	0.37	46.6	0.066
	C4	4	0.43	0.40	43.8	0.072
	C5	5	0.39	0.22	33.4	0.029
	C6	6	0.20	0.14	27.3	0.008
0.1	A2	2	0.28	0.23	38.3	0.024
	A3	3	0.30	0.39	29.6	0.035
	A4	4	0.34	0.47	34.3	0.055
	A5	5	0.33	0.34	42.0	0.048
	A6	6	0.38	0.33	31.3	0.032
0.5	B2	2	0.24	0.10	39.9	0.010
	B3	3	0.31	0.25	37.8	0.030
	B4	4	0.28	0.18	43.4	0.023
	B5	5	0.25	0.19	34.3	0.016
	B6	6	0.29	0.11	37.5	0.012

this point, it can be assumed that saturation of QDs has been achieved. This observation is in-line with the work by Deepa et al. [19]. Also noted that the J-V curves have minor peak near the open circuit voltage, which indicates possible presence of pin hole in the sample.

Samples prepared from 0.1 M precursor concentration shows a similar pattern in which the best performing device is achieved when the sample was prepared with 4 SILAR cycles. Such sample has V_{OC} value of 0.34 V, J_{SC} value of 0.47 mA/cm^2, fill factor (FF) value of 34.3%, and efficiency of 0.055%. As for the samples prepared from 0.5 M precursor concentration, sample prepared with 3 SILAR cycles exhibit the best overall performance. It has V_{OC} of 0.31 V, J_{SC} of 0.25 mA/cm^2, and efficiency of 0.030%. All the samples exhibit a relatively low value of FF, which is less than 50%. This signifies a substantial charge recombination which needs to be tackled with. One of the remedies is to apply passivation layer [20].

On the other hand, samples prepared from higher precursor concentration have lower efficiency as higher precursor concentration leads to multiple nucleation sites for QD growth. Eventually, more QDs are formed until blocking the TiO_2 interface pathway. Thus, the thickening of SnS QD layers results in the impediment of electrons transfer across the interface. Meanwhile, V_{OC} was observed to increase with incremental of SILAR dipping cycles, up to optimum dipping cycle. The increased of V_{OC} is due to the increase of Fermi level of the photoelectrode with the presence of SnS QDs, allowing more injection of electrons from SnS QDs to the TiO_2 layer. Upon reaching the optimum parameter limits, J_{SC} and V_{OC} of the samples reduced which are due to the decrease in electrons recombination resistance in the devices led by overloading of SnS on the surface of TiO_2 layer. Overloading of SnS sensitizer also causes the reduction of V_{OC} and FF because it blocks the electrolyte penetration into the porous thin film [21]. One of the major contributing factors to the low performance of solar cell is the high charge recombination rate. Although impedance spectroscopy was not performed, judging from the performance parameters (as shown in Table 2), one can predict the low electrons recombination resistance within the interfaces of the samples. Such phenomenon can result in high charge transfer resistance R_{ct} with small capacitance Cμ, signifying slow charge transport at the interfaces. Ultimately, their electron lifetime values would be at the low side, demonstrating ineffective electrons transfer, which result in lower energy conversion efficiency [22-25].

In the later stage, SnS QDSSC devices with the best parameter performances determined from I-V test were selected for UV-Vis absorption analysis in order to estimate the bandgap energy of the QD. Other samples were not tested for their absorption as the value from the best performing sample in each set is sufficient to provide the necessary information. Absorption spectra of TiO_2/SnS thin film with different concentration and SILAR cycles are shown in Figure 4a. The bandgap of samples are determined by extrapolating the Tauc plot to x-axis as shown in Figure 4b (for selected samples A4, B3 and C4).

Absorption spectra of TiO_2/SnS samples increased as the number of SILAR cycle increased. Also, the absorbance is higher for samples fabricated with higher

precursor solution concentration. This is due to more SnS QDs formed on the TiO_2 layer which allow more light absorption. From Tauc plot analysis, samples with more SILAR cycles tend to have lower bandgap energy. The bandgap energy values for the selected samples are tabulated in Table 3. It is also observed that bandgap energy is also increased with the increasing deposition concentration except for samples prepared from 0.5 M precursor concentration.

The QD size was estimated from the absorption spectrum according to reported method [9]. The bulk bandgap energy for SnS is 1.3 eV, according to Deepa et al. [19]. The SnS QDs sizes increased with more SILAR cycles in each set of samples with the same concentration. For example, TiO_2/SnS samples prepared from 0.05 M precursor solution, the size of SnS QDs increased from 6.68 nm to 8.39 nm when the number of cycles increased from 4 to 6 cycles. This shows the quantum confinement effect as the dipping cycle and precursor concentration increased. By comparing among the different precursor concentration, there is an optimum QD size with its corresponding bandgap for the best device performance. The reduction of performance with higher QD size could be linked to the thickening layer of the QDs which reduce the charge recombination resistance within the interface [26].

Table 3: SnS QD size and its corresponding bandgap energy.

Concentration (M)	Sample ID	Bandgap energy (eV)	QD radius (nm)
0.05M	C2	1.77	6.31
	C3	1.73	6.52
	C4	1.71	6.68
	C5	1.63	7.45
	C6	1.56	8.39
0.1M	A2	1.80	6.25
	A3	1.79	6.27
	A4	1.75	6.38
	A5	1.71	6.69
	A6	1.68	7.06
0.5M	B2	1.69	7.00
	B3	1.67	7.03
	B4	1.62	7.55
	B5	1.60	7.68
	B6	1.58	8.46

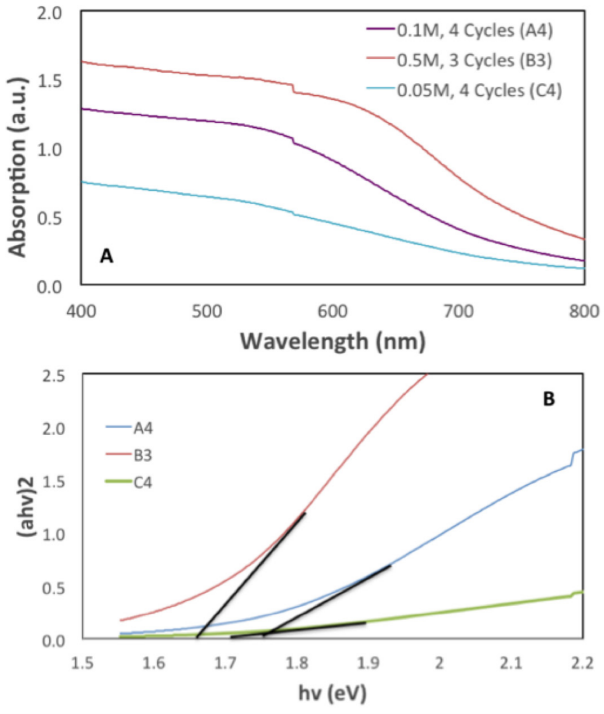

Figure 4: (a) Absorption spectra of selected samples of TiO_2/SnS multilayer film; (b) Tauc plots of selected samples of TiO_2/SnS multilayer film.

As the overall performance of the cells is still very low, plan is under way for optimization study. Although other semiconductor QD materials like CdS, CdSe and PbS have shown better performance, SnS being less toxic than the usual QD materials could have a better future application should more effort on optimization work is carried out. It must also be noted that the assembly cell samples in this work used generic setup in order to eliminate other positive contributing effect to the result, unlike other reported result in literature where optimized setup has been used. Some of the parameters that need to be focused on include dipping time and different precusor used. The deposition of blocking layer and passivation layer are also crucial for the better performance of the cells, which are not being applied in this preliminary study. Optimized electrolyte should also be looked into as different semiconductor QDs could perform well in different composition of polysulfide electrolyte [27,28]. Lastly, suitable counter electrode materials should also be considered. Typically, Cu_2S counter electrode produces better result when used in QDSSC [29-32].

4 Conclusion

Tin (II) sulfide QDSSCs have been successfully fabricated using SILAR method from aqueous solution. SEM and EDX analysis on TiO_2/SnS surface showed the presence of SnS nanoparticles attached to the TiO_2 particles. The devices performances were characterized using

I-V tester and solar simulator. The overall efficiency of SnS QDSSCs increased when the concentration of precursor solution for QDs fabrication decreased from 0.5 M to 0.05 M. For a fixed precursor concentration, the efficiency of QDSSCs reduced once the optimal SILAR cycles were achieved. Further increasing the SILAR cycles did not increase the conversion efficiency of QDSSCs due to overloading of QDs where the aggregates would obstruct the electron transfer through the interface. The optimum SILAR cycles for 0.05 M and 0.1 M precursor concentration were 4 cycles, while for 0.5 M, optimum SILAR cycle was 3 cycles. The best performance was obtained from sample prepared from 0.05 M concentration, 4 SILAR cycles. Although the performance is relatively low, this work shows the feasibility of SnS QDs as alternative green material for QDSSC devices.

Acknowledgments: The authors are grateful for the research fund provided by the Ministry of Higher Education (MOHE) of Malaysia under the Fundamental Research Grant Scheme no. FRGS/1/2015/SG06/UTAR/02/1.

References

[1] Jun H.K., Careem M.A., Arof A.K., Quantum dot-sensitized solar cells—perspective and recent developments: A review of Cd chalcogenide quantum dots as sensitizers. Renew. Sust. Energy Rev., 2013, 22, 148-167.

[2] Green M.A., Silicon Photovoltaic Modules: A Brief History of the First 50 Years. Prog. Photovolt: Res. Appl., 2005, 13, 447-455.

[3] Shah A., Torres P., Tscharner R., Wyrsch N., Keppner H., Photovoltaic Technology: The Case for Thin-Film Solar Cells. Science, 1999, 285, 692-698.

[4] Grätzel M., Photoelectrochemical cells. Nature, 2001, 414, 338-344.

[5] Shockley W., Queisser H.J., Detailed Balance Limit of Efficiency of p-n Junction Solar Cells. J. Appl. Phys., 1961, 32, 510-519.

[6] Duan J., Zhang H., Tang Q., He B., Yu L., Recent advances in critical materials for quantum dot-sensitized solar cells: a review. J. Mater. Chem. A, 2015, 3, 17497-17510.

[7] Rühle S., Shalom M., Zaban A., Quantum-Dot-Sensitized Solar Cells. ChemPhysChem, 2010, 11, 2290-2304.

[8] Ristov M., Sinadinovski G.J., Grozdanov I., Chemical deposition of Cu_2O thin films. Thin Solid Films, 1985, 123, 63-67.

[9] Jun H.K., Careem M.A., Arof A.K., Fabrication, Characterization, and Optimization of CdS and CdSe Quantum Dot-Sensitized Solar Cells with Quantum Dots Prepared by Successive Ionic Layer Adsorption and Reaction. Int. J. Photoenergy, 2014, Article ID 939423.

[10] Deepa K.G., Sunil M.A., Nagaraju J., SnS quantum dot solar cells with Cu2S as counter electrode. IEEE 38th Photovoltaic Specialists Conference, 2012, 000798-000800.

[11] Hortikar S.S., Kadam V.S., Rathi A.B., Jagtap C.V., Pathan H.M., Mulla I.S., et al., Synthesis and deposition of nanostructured SnS for semiconductor-sensitized solar cell. J. Solid State Electrochem., 2017, 21, 2707-2712.

[12] Zhang X.-P., Lan Z., Chen L., Gao S.-W., Wu W.-X., Que L.-F., et al., Preparation and photovoltaic performance of SnS sensitized nanocrystallite TiO_2 photoanode. J. Inorg. Mater., 2013, 28, 1093-1097.

[13] Liu I.-P., Chang C.-W., Teng H., Lee Y.L., Performance Enhancement of Quantum-Dot-Sensitized Solar Cells by Potential-Induced Ionic Layer Adsorption and Reaction. ACS Appl. Mater. Interfaces, 2014, 6, 19378-19384.

[14] Mehrabian M., Mirabbaszadeh K., Afarideh H., Solid-state ZnS quantum dot-sensitized solar cell fabricated by the Dip-SILAR technique. Phys. Scr., 2014, 89, 085801.

[15] Ha T.T., Lam Q.V., Huynh T.D., Quantum dots-sensitized solar cell: SILAR cycles effect on the parameters of photovoltaic. Int. J. Latest Res. Sci. Tech., 2014, 3, 127-132.

[16] Guo W., Shen Y., Wu M., Wang L., Wang L., Ma T., SnS-Quantum Dot Solar Cells Using Novel TiC Counter Electrode and Organic Redox Couples. Chem.-Eur. J., 2012, 18, 7862-7868.

[17] Deepa K.G., Nagaraju J., Growth and photovoltaic performance of SnS quantum dots. Mater. Sci. Eng. B, 2012, 177, 1023-1028.

[18] Mora-Sero I., Gimenez S., Fabregat-Santiago F., Gomez R., Shen Q., Toyoda T., et al., Recombination in Quantum Dot Sensitized Solar Cells. Acc. Chem. Res., 2009, 42, 1848-1857.

[19] Deepa K.G., Nagaraju J., Development of SnS quantum dot solar cells by SILAR method. Mater. Sci. Semicond. Process., 2014, 27, 649-653.

[20] Lan X., Voznyy O., Kiani A., Garcia de Arquer F.P., Abbas A.S., Kim G.H., et al., Passivation Using Molecular Halides Increases Quantum Dot Solar Cell Performance. Adv. Mater., 2016, 28, 299-304.

[21] Tsukigase H., Suzuki Y., Berger M.H., Sagawa T., Yoshikawa S., Synthesis of SnS Nanoparticles by SILAR Method for Quantum Dot-Sensitized Solar Cells. J. Nanosci. Nanotech., 2011, 11, 1914-1922.

[22] Kim H.-J., Xu G.-C., Gopi C.V.V.M., Seo H., Venkata-Haritha M., Shiratani M., Enhanced light harvesting and charge recombination control with TiO_2/PbCdS/CdS based quantum dot-sensitized solar cells. J. Electroanal. Chem., 2017, 788, 131-136.

[23] Gopi C.V.V.M., Venkata-Haritha M., Seo H., Singh S., Kim S.-K., Shiratani M., et al., Improving the performance of quantum dot sensitized solar cells through CdNiS quantum dots with reduced recombination and enhanced electron lifetime. Dalton Trans., 2016, 45, 8447-8457.

[24] Samadpour M., Improving the parameters of electron transport in quantum dot sensitized solar cells through seed layer deposition. RSC Adv., 2018, 8, 26056-26068.

[25] Wu Q., Hou J., Zhao H., Liu Z., Yue X., Peng S., et al., Charge recombination control for high efficiency CdS/CdSe quantum dot co-sensitized solar cells with multi-ZnS layers. Dalton Trans., 2018, 47, 2214-2221.

[26] Mora-Seró I., Giménez S., Moehl T., Fabregat-Santiago F., Lana-Villareal T., Gómez R., et al., Factors determining the photovoltaic performance of a CdSe quantum dot sensitized solar cell: the role of the linker molecule and of the counter electrode. Nanotech., 2008, 19, 424007.

[27] Jun H.K., Careem M.A., Arof A.K., A Suitable Polysulfide Electrolyte for CdSe Quantum Dot-Sensitized Solar Cells. Int. J. Photoenergy, 2013, Article ID 942139.

[28] Lee Y.L., Chang C.-H., Efficient polysulfide electrolyte for CdS quantum dot-sensitized solar cells. J. Power Sources, 2008, 185, 584-588.

[29] Hessein A., Wang F., Masai H., Matsuda K., El-Moneim A.A., Improving the stability of CdS quantum dot sensitized solar cell using highly efficient and porous CuS counter electrode. J. Renew. Sust. Energy, 2017, 9, 023504.

[30] Gopi C.V.V.M., Ventaka-Haritha M., Kim S.-K., Kim H.-J., Facile fabrication of highly efficient carbon nanotube thin film replacing CuS counter electrode with enhanced photovoltaic performance in quantum dot-sensitized solar cells. J. Power Sources, 2016, 311, 111-120.

[31] Gopi C.V.V.M., Ravi S., Rao S.S., Reddy A.E., Kim H.-J., Carbon nanotube/metal-sulfide composite flexible electrodes for high-performance quantum dot-sensitized solar cells and supercapacitors. Sci. Rep., 2017, 7, 46519.

[32] Jun H.K., Careem M.A., Arof A.K., Performances of some low-cost counter electrode materials in CdS and CdSe quantum dot-sensitized solar cells. Nanoscale Res. Lett., 2014, 9, 69.